INACTIVATION OF VOLTAGE-GATED DELAYED POTASSIUM CURRENT IN MOLLUSCAN NEURONS

A KINETIC MODEL

RICHARD W. ALDRICH, *Department of Biological Sciences, Stanford University, Hopkins Marine Station, Pacific Grove, California 93950*

ABSTRACT Voltage-gated delayed potassium current in molluscan neurons is characterized by a marked inactivation. Inactivation can accumulate between repetitive pulses, giving rise to current patterns in which the maximum current during a second voltage pulse is less than the current at the end of the preceding pulse (cumulative inactivation). Other features of inactivation of this current include an onset time-course that can be characterized by the sum of two exponential processes and an early minimum in the recovery-vs.-time curve. A simple four-state model is developed that can, when supplied with rate constants derived from voltage-clamp experiments, reproduce these features of inactivation. The model incorporates state-dependent inactivation rates. Upon depolarization, both open and closed channels can be inactivated, although inactivation of closed channels is much faster. Upon repolarization, recovery from inactivated states is sufficiently slow that little recovery occurs during a short interpulse interval. Cumulative inactivation comes about as a result of fast inactivation during the second pulse, further limiting the peak current from the level at the end of the previous pulse.

INTRODUCTION

Inactivation of the potassium channels responsible for delayed rectification has been described in a wide variety of excitable cells: Squid axon (Ehrenstein and Gilbert, 1966); amphibian axon (Frankenhaeuser, 1963, Schwarz and Vogel, 1971); skeletal muscle (Nakajima et al., 1962; Adrian et al., 1970 *a, b*); vertebrate neurons (Nakajima, 1966); and molluscan neurons (Hagiwara et al., 1961, Connor and Stevens, 1971*a;* Lux and Eckert, 1974).

The presence of a calcium-activated potassium current in molluscan neurons has complicated the analysis of voltage-gated delayed rectification in these cells (Meech and Standen, 1975; Thompson, 1977). With techniques to isolate the voltage-gated current from the calcium-gated current, the inactivation of the voltage-gated potassium current (I_K) has been studied and characterized in the marine molluscs *Archidoris* and *Anisodoris* (Aldrich et al., 1979). The following features of inactivation of this current were described: (*a*) during a long voltage pulse, the current inactivates to a nonzero steady-state level. (*b*) During repetitive voltage pulses of short duration, the maximum current during the second pulse is often less than the amplitude at the end of the first pulse (cumulative inactivation). This difference decreases with successive pulses until a steady state is reached. (*c*) The development of

---

Dr. Aldrich's present address is Department of Physiology, Yale School of Medicine, New Haven, Connecticut 06510.

inactivation during a prepulse can be characterized by the sum of two exponentials. (*d*) Recovery from inactivation is slow, requiring as much as a few minutes for complete recovery. (*e*) There is a short time after the end of a voltage pulse when inactivation of peak current during a second pulse increases with time, causing an early minimum in the recovery-vs.-time curve.

These complexities in kinetics suggest something other than a simple, voltage-dependent, first-order transition between single open and closed states of the channel. Multiple-state kinetic schemes have been devised to account for similar complex properties of the kinetics of sodium channels (Chandler and Meves, 1970; Armstrong and Bezanilla, 1977; Chiu, 1977), and for potassium current inactivation (Kostyuk et al., 1976). In an earlier paper (Aldrich et al., 1979), we suggested that cumulative inactivation during repeated voltage pulses and the early minimum in the recovery-vs.-time curve could be explained by a kinetic model involving state-dependent inactivation rates. This concept implies a multistate model for the voltage-gated potassium channel. It is shown here that a mathematical formulation of such a model can reproduce the features of inactivation of delayed outward current in molluscan neurons.

METHODS

Experimental methods for voltage clamp of isolated dorid neuronal somata are presented in detail in a previous publication (Aldrich et al., 1979). The voltage-dependent delayed outward current was isolated by bathing the cell in artificial sea water in which 10 mM cobalt chloride was substituted for calcium chloride to eliminate the calcium-dependent current. Cells with a large contribution of voltage-dependent potassium current were used to minimize error due to incomplete block of the calcium-dependent potassium current by cobalt.

Computer modeling was carried out on a PDP 11-03 laboratory computer equipped with a VT-55 plotting terminal (Digital Equipment Corp., Marlboro, Mass.). Standard numerical integration techniques were used. Results were photographed directly from the terminal screen. A slight upward curvature in the base line can be seen in some records as a result of a slight curvature of the screen.

RESULTS

Properties of Voltage-gated Delayed Outward Current

Typical voltage-clamp records from the isolated soma of a neuron from the marine mollusc *Archidoris* or *Anisodoris* are shown in Fig. 1. The cell was bathed in calcium-free cobalt solution to isolate the voltage-gated outward current (Thompson, 1977; Aldrich et al., 1979). At the holding potential (−40 mV) the transient outward current studied by Hagiwara et al. (1961), Neher (1971), and Connor and Stevens (1971*b*) is inactivated. Panel *A* shows the delayed rectifier current in response to a voltage step from −40 to +15 mV. The current increases rapidly to a peak and then declines to a nonzero steady-state level. Leakage current at this voltage contributes only a small amount of current to the steady-state level. Panel *B* shows currents recorded during a series of 400-ms voltage pulses from −40 to +15 mV. This record illustrates the accumulation of inactivation between pulses. The peak current during the second pulse is less than the current at the end of the first pulse. The difference is greatest between the first two pulses and decreases with further pulses until a steady-state current waveform is reached. The outward tail currents at the end of each voltage pulse decrease in

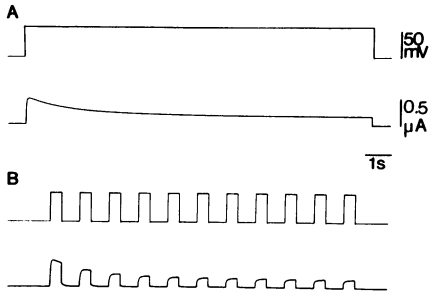

FIGURE 1 Voltage-gated delayed outward current in the isolated soma of a neuron of *Archidoris* or *Anisodoris*. (*A*) Outward current in response to a 13-s depolarization from a holding voltage of −40 to +15 mV. The current rises to a peak and then slowly inactivates to a steady-state level. (*B*) Repetitive 400-ms voltage steps to the same voltage at a frequency of 1 pulse/s. Cumulative inactivation can be seen between pulses. Solution (in mM) NaCl, 470; KCl, 10; $MgCl_2$, 50; Tris Cl, 10; $CoCl_2$, 10.

magnitude with repetitive pulses as a result of the inactivation of the channels. Accumulation of extracellular potassium is not the major reason for the decline in outward current, as a large amount of inactivation can be seen with no change in the reversal potential for the current, which indicates that no significant accumulation of external potassium has occurred (Aldrich et al., 1979). Potassium accumulation does occur in these cells for long pulses, however, causing a depression of outward current that can lead to an overestimation of the amount of inactivation of permeability.

Some of these features of outward current in molluscan neurons have been described by numerous authors: Alving, 1969; Leicht et al., 1971; Connor and Stevens, 1971*a, c;* Neher and Lux, 1971; Magura et al., 1971; Gola, 1974; Kostyuk et al., 1975, 1976; Heyer and Lux, 1976*a, b*. Recovery from inactivation is very slow and is characterized by an increase in inactivation of current during a second voltage pulse at times $<\sim 1$ s after a first pulse. (Neher and Lux, 1971; Kostyuk et al., 1975; Eckert and Lux, 1977). By using techniques that virtually eliminate the contribution of the fast-transient (I_A) and calcium-dependent (I_C) outward currents, all of the above features were found to be properties of the voltage-dependent delayed potassium current (I_K) (Aldrich et al., 1979).

A Kinetic Model for Inactivation of I_K

It has been shown (Aldrich et al., 1979) that the development of inactivation of outward current during a prepulse can be approximated by the sum of two exponential processes with time constants differing by almost an order of magnitude (570 ms and 3.45 s at 0 mV). A simple kinetic scheme that will give rise to this type of behavior would be two voltage-dependent inactivation processes occurring during the prepulse. A specific case would be that the two time constants of inactivation are taken to be separate processes for the inactivation of either closed or open channels. The rate of inactivation depends upon the state of the channels, i.e., closed channels have a higher probability of inactivating during a voltage step than do open channels; therefore, inactivation of closed channels is faster than inactivation of open channels.

According to this scheme a channel can exist in one of four states, shown in the following

diagram:

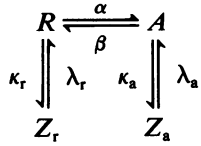

R is the resting state of the channel, A is the activated (and only conducting) state, and Z_r and Z_a are the two inactivated states. The transition-rate constants among the various states are as follows:

- κ_r fast inactivation of closed channels
- λ_r slow recovery from fast inactivation
- κ_a slow inactivation of open channels
- λ_a slow recovery from slow inactivation of open channels
- α opening of closed channels
- β closing of open channels

The rate constants are functions of transmembrane potential. A transition between the two inactivated states Z_r and Z_a was not included for simplicity because no data exist at this time to determine its presence. It is possible that it may need to be included to explain future voltage-clamp results. By not including this hypothetical transition, the introduction of an arbitrary rate constant into the model was avoided.

The kinetic model behaves in the following way: when a depolarizing voltage change occurs, closed resting channels either open or become inactivated by the fast process. This can be thought of as a competition of the two processes, in that a channel that opens cannot undergo fast inactivation and a channel that is inactivated by this means cannot open. This limits the peak permeability during the voltage pulse. The fast inactivation that occurs before peak current will cause the permeability at the peak to be considerably less than the maximum permeability that would be available at that voltage if resting channels did not inactivate. Channels that open are subject to the slow inactivation process, and the current declines to a steady state.

Cumulative inactivation comes about from interaction of the fast inactivation process and the slow recovery. Because of the slow recovery, channels inactivated during the first pulse of a pair are unavailable for reactivation during a second pulse that occurs after a short interval. As a result of fast inactivation during the second pulse, the number of channels available for activation during the pulse is further limited, causing the peak current during the second pulse to be less than the current at the end of the first pulse. With successive pulses this process continues as channels accumulate in the inactive states.

Numerical Solution of the Four-state Model

On the assumption of a constant number of channels, the four-state model gives rise to the following system of differential equations:

$$\frac{d(A)}{dt} = \alpha(R) + \lambda_a(Z_a) - \beta(A) - \kappa_a(A), \tag{1}$$

$$\frac{d(Z_r)}{dt} = \kappa_r(R) - \lambda_r(Z_r), \tag{2}$$

$$\frac{d(Z_a)}{dt} = \kappa_a(A) - \lambda_a(Z_a), \tag{3}$$

$$\frac{d(R)}{dt} = \beta(A) + \lambda_r(Z_r) - \kappa_r(R) - \alpha(R), \tag{4}$$

where (A), (Z_r), (Z_a), and (R) are the proportion of channels in the respective states.

Current waveforms can be calculated from the following equation:

$$I_K = \bar{g}_K(A)(V - V_{REV}), \tag{5}$$

where $\bar{g}_K$ is the maximum conductance for I_K, and V_{REV} is the reversal potential for I_K. This relationship implies that the instantaneous current-voltage relationship is linear. The instantaneous *I-V* curve in these cells shows a slight outward curvature. Owing to the inaccuracies in the determination of the shape of the curve in the presence of residual unblocked calcium-dependent outward current, this assumption seems reasonable. Numerical solutions of Eqs. 1–5 were performed using values of parameters obtained from voltage-clamp data published previously (Aldrich et al., 1979).

Solution of the Model Using Experimentally Derived Rate Constants

The values of the various rate constants were derived in the following way: the kinetic measurements from Figs. 9 and 11 of Aldrich et al. (1979) were used, along with the average values we found for time-to-peak, steady-state-to-peak ratio, and tail-current relaxation time constants. In general, experimentally measured time constants were taken to be the reciprocals of the forward rate constants for the transition between the relevant states. In this way:

$1/\kappa_r$ = fast inactivation time constant at $V = +20.0$ mV,

$1/\lambda_r$ = recovery time constant at $V = -40$ mV,

$1/\alpha$ = activation time constant at $V = +20$ mV,

$1/\beta$ = tail-current time constant at $V = -40$ mV.

This method neglects the contribution of the backward rate constant to the measured time constant, a simplification that implies that the voltage dependence of the transition is steep enough that the forward transition is highly favored during a depolarizing step, whereas the opposite transition is highly favored at holding voltage. This departs from reality where the forward and backward transition rate constants would be continuously dependent upon voltage. It allows, however, in the absence of detailed data on the voltage dependence of each rate constant, a simple way of assigning values to the rate constants for large depolarizing steps. The small contribution of λ_r (which was made independent of voltage) to the fast inactivation time constant was ignored.

Both forward and backward transitions were considered in the assignment of values to the rate constants λ_a and κ_a. The quantity $1/(\lambda_a + \kappa_a)$ was held approximately equal to the slow inactivation time constant, while the values of λ_a and κ_a were adjusted to obtain a suitable steady-state current level. Once all of the other rate constants were set, α was adjusted to give a reasonable time-to-peak current. The values for all the rate constants at both holding voltage (-40 mV) and pulse voltage (20 mV), and the details of assigning their values from voltage-clamp data, are given in Table I. The reversal potential for I_K was made -60 mV. The initial conditions were such that all channels were in state R at -40.0 mV at steady state.

Simulations of the system with this set of rate constants are shown in Fig. 2 for both a long

TABLE I
VALUES OF RATE CONSTANTS DERIVED FROM EXPERIMENTAL DATA

	Voltage		Voltage-clamp data*
	Holding (−40.0 mV)	Pulse (20.0 mV)	
	(s^{-1})		
κ_r	0.0	2.0	Fast inactivation, Fig. 9
λ_r	0.03	0.03	Recovery, Fig. 11
β	20.0	0.0	Tail currents at −40 mV
α	0.0	10.0	Adjusted to give time to peak
λ_a	0.03	0.09	Recovery, Fig. 11‡
κ_a	0.0	0.24	Slow inactivation, peak-to-steady-state ratio, Fig. 9‡

*For details and figures, see Aldrich et al. (1979).
‡The values of λ_a and κ_b at $V = 20$ mV were obtained by keeping the ratio $1/(\lambda_a + \kappa_a) \simeq 3$ s (Fig. 9) while adjusting their values to arrive at a suitable steady-state-to-peak ratio.

(15 s) pulse and repetitive 0.5-s pulses at 1 pulse/s. The results show that: (*a*) The current rises and inactivates to a nonzero steady-state level; (*b*) upon repetitive pulses, the currents continue to inactive until a steady state is reached; (*c*) the tail currents inactivate with repetitive pulses; and (*d*) cumulative inactivation occurs. A comparison with voltage-clamp records of I_K in Fig. 1 shows that the four-state model can adequately reproduce the properties of I_K.

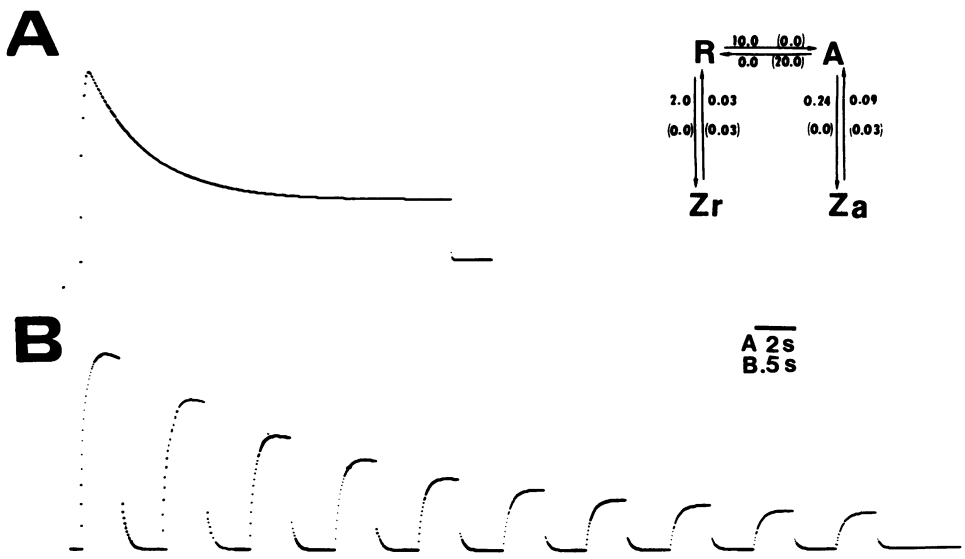

FIGURE 2 Results of computer simulations using the four-state model with the rate constants listed in Table I. (*A*) Simulated current recorded during a 15-s pulse from −40 to 20 mV. The current rises to an early peak and inactivates to a nonzero steady state. (*B*) Simulated currents recorded during 500-ms pulses repeated once per second. The features of cumulative inactivation are present. Time scale in (*A*) is four times slower than in (*B*). The inset shows the rate constants used. The values in parentheses are those at hold voltage. Those not in parentheses are the value at 20 mV. Time scale: (*A*) 2 s. (*B*) 500 ms.

A more detailed look at the transitions between the four states that underlie the current waveforms is shown in Fig. 3. At the top of the figure are current waveforms for paired voltage pulses with the same rate constants as in Fig. 2. Under the current waveforms are the relative occupancies of each of the four states during the same voltage pulses. State A is proportional to the conductance. The accumulation of inactivation can be be seen in the occupancy of both states Z_r and Z_a. The proportion of channels in the inactive states rises during the first pulse but decays slowly between pulses. The increment in the proportion of inactivated channels during the second pulse is less for both states Z_r and Z_a, which signifies, respectively, the decline in cumulative inactivation and the inactivation rate during successive pulses. Two phases of recovery of closed channels after a pulse can be seen by examining the time-course of state R. At the end of the first pulse, there is a relatively fast increase in state R followed by a much slower increase. The early fast increase is due to the time-dependent closing of open channels and is reflected in the current waveforms as the tail current. The slow increase is the recovery from inactivated states. After the second pulse, this recovery starts from a lower value because of the accumulation of channels in the inactivated states due to the first pulse.

Analysis of the Recovery Curve in Terms of the Four-state Model

One of the features of inactivation of I_K is an early phase of increasing inactivation in the recovery-vs.-time curve. If the four-state model is an accurate representation of the kinetics of

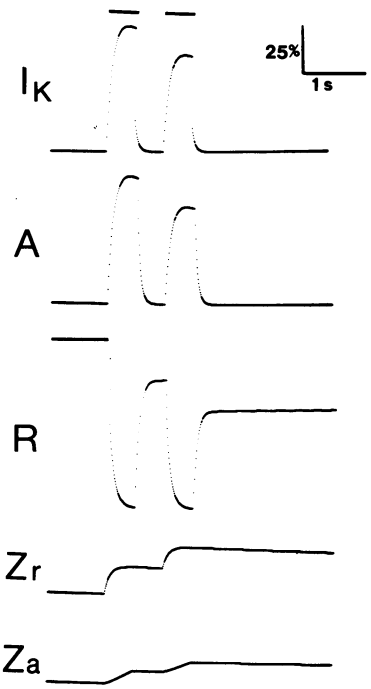

FIGURE 3 Relative occupancy of the four states of the model during paired pulses. The first two current waveforms of Fig. 2 *B* are reproduced (I_K). The lines above the waveforms indicate the periods where the voltage was stepped to +20 mV from a holding voltage of −40 mV. The four traces below the current waveforms show the relative occupancy of the four states of the model; activated (A), resting (R), and the two inactivated states (Z_r and Z_a).

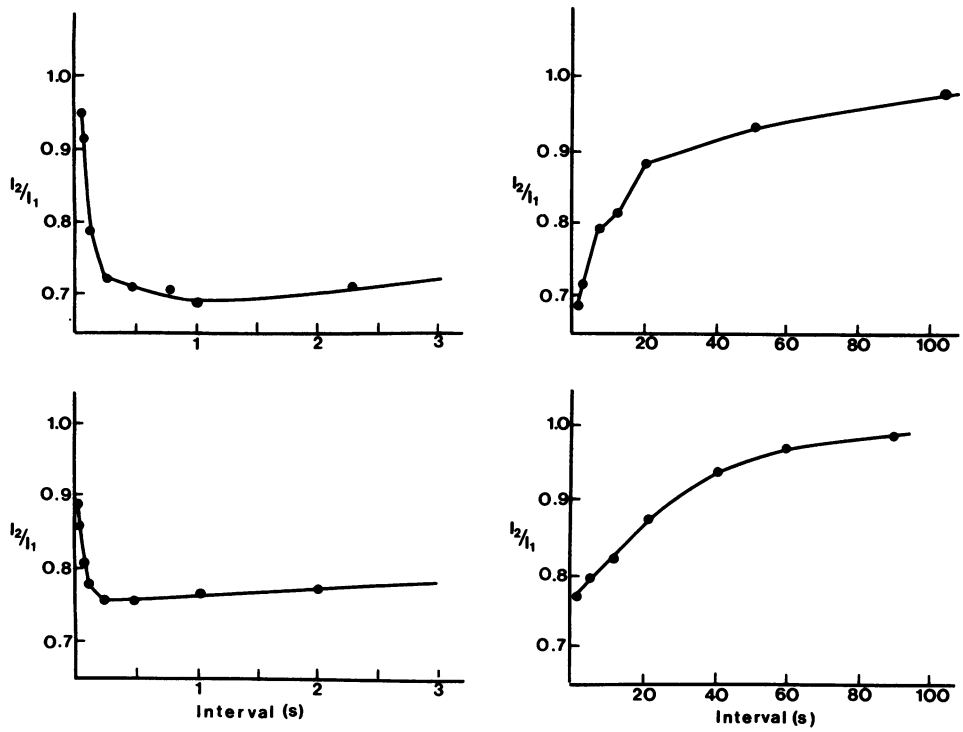

FIGURE 4 Recovery curves for I_K (top) and the four-state kinetic model. The rate constants used are those from Table I and Fig. 2. The recovery curves for I_K in the top half of the figure are those of Fig. 11 of Aldrich et al. (1979).

I_K, it should reproduce this phenomenon. The lower half of Fig. 4 showns the results of a computer simulation in which paired voltage pulses were separated by a varying interval with no adjustment of rate constants from those used in Fig. 2. The ratio of peak currents (I_2/I_1) is plotted vs. the length of the interval similar to the experiment of Fig. 11 in Aldrich et al. (1979). The results of that figure are reproduced on the top half of Fig. 4, so that a direct comparison can be made. As can be seen, the simulated recovery curve is very similar to that obtained by voltage-clamp experiments in that both have a minimum at times earlier than 1 s, followed by a slow recovery over many seconds. No attempt was made to match exactly the shape of the experimental recovery curve by varying the values of the rate constants. It should be emphasized, however, that both current waveforms and the general form of the recovery curve are easily obtained from a single set of experimentally derived rate constants.

In terms of the four-state model, a mechanism for the shape of the recovery curve can be studied. It can be seen by the state diagram that the amount of fast inactivation depends upon the number of resting channels. After a single pulse, the channels that are open do not instantaneously close; the tail current reflects the time-course of the closing of these channels. During the tail, the channels that remain open cannot undergo fast inactivation at the occurrence of a second voltage step. Thus, less fast inactivation will occur during a voltage pulse presented during a tail current than will occur during a pulse presented after the tail is over. Because of this "protection" from inactivation, currents recorded during a second pulse

presented during the tail will be larger than those occurring during a second pulse presented after its completion. The falling phase of the recovery curve can be accounted for by this process. In Fig. 5, the occupancy of state Z_r is shown for paired pulses at various intervals. It can be seen that as the interval decreases, the amount of fast inactivation during the second pulse decreases. The decrease is dramatic when the second pulse occurs during the time-course of the tail current following the first pulse, showing the protection from fast inactivation during the tail.

Solution of the Model Using Arbitrary Rate Contants

In the foregoing, the major kinetic properties of I_K currents have been reproduced by a simple model that utilizes first-order transitions of channels between open, closed, and inactivated

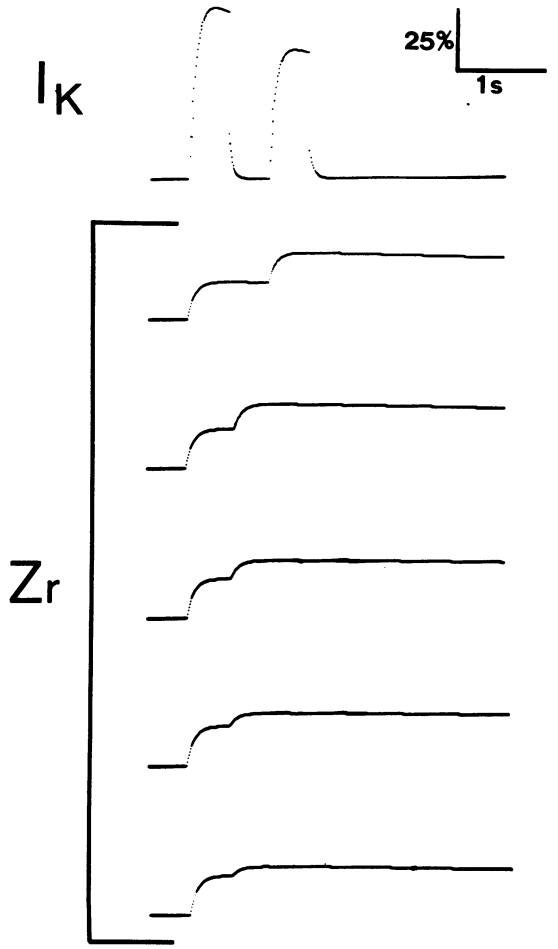

FIGURE 5 The effect of the length of the interpulse interval on fast inactivation during the second pulse. The two pulses are 500 ms in duration with variable interpulse interval. Below the current waveforms are traces showing the relative occupancy of the inactivated-closed state of the model (Z_r) similar to Fig. 3. The occupancy of this state during the second pulse is a reflection of fast inactivation during that pulse. The magnitude of fast inactivation during the second pulse decreases dramatically when the second pulse occurs during the tail current following the first pulse. Rate constants from Table I.

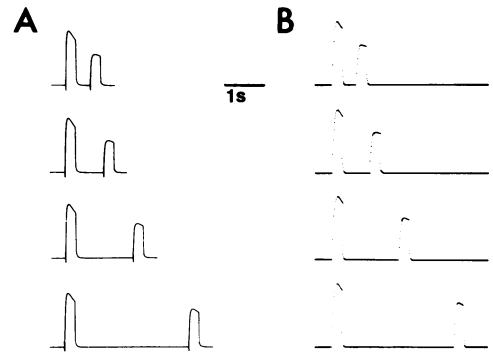

FIGURE 6 Comparison of current waveforms (*A*) and numerical solutions of the four-state model (*B*). Rate constants, arbitrarily chosen to produce the fit shown in the top row, are given in Table II. The interpulse interval was increased without changing any rate constants to produce the solutions in the lower three rows.

states. It should be recognized that there is considerable variability in the outward current patterns of different cells. Although a large part of this can be accounted for by a difference in the ratios of Ca-activated and voltage-dependent current, there also seems to be a difference in the I_K system. In Ca-free cobalt solution, differences in magnitude of current, activation and inactivation rates, and steady-state-to-peak ratios can be seen (Reuter and Stevens, 1980). The interpretation of this variability in I_K kinetics is made more difficult by the incomplete block of I_C by Ca-free cobalt solution (Aldrich et al., 1979). Given these differences, and the unknown contributions of series resistance error and external potassium accumulation to the voltage clamp records, it is unreasonable to expect exact replication of experimental current waveforms by the four-state model with rate constants derived from measurements of the currents on a variety of cells.

All of the results presented have used a set of rate constants derived from experimental measurements of outward currents from a population of cells. If greater freedom is allowed in the selection of rate constants, a close fit to the current waveforms of a particular cell can be produced. For the calculated current waveforms in Fig. 6 *B*, the rate constants were arbitrarily chosen to produce records similar to the voltage-clamp records in Fig. 6 *A* for the shortest interval shown between two pulses. These rate constants are listed in Table II. Once

TABLE II
RATE CONSTANTS USED TO FIT CURRENT WAVEFORMS IN FIG. 6

	Voltage	
	−40.0	+2.0
	(s^{-1})	
κ_r	0.0	8.0
λ_r	0.07	0.03
β	40.0	0.0
α	0.0	0.0
λ_a	0.07	2.0
κ_a	0.0	1.2

the rate constants were set, current waveforms were computed for paired voltage pulses with increasing interpulse intervals, with no further change in the rate constants. The calculated current waveforms can be compared to the experimental records in panel *A*. The peak current amplitude and the amount of inactivation during the second pulse can be seen to recover similarly with increasing interpulse interval. The model adequately reproduces current waveform for the longer intervals even though the rate constants were chosen to reproduce the current records at the shortest interval. The close similarity between the experimental and theoretical results illustrates the fact that the model can be made to closely fit data from a single cell.

DISCUSSION

The results presented here have shown that a simple four-state model can predict many of the kinetic features of I_K. By using rate constants that are for the most part derived from the results of voltage-clamp experiments, the properties of the inactivation of this current can be reproduced.

It is important to realize that the kinetic features of I_K have been obtained from a fairly simple model that uses first-order transitions between various states of the channel. No novel mechanism, such as continued inactivation during the interpulse interval, was needed to explain cumulative inactivation. In addition, little adjustment of parameters was necessary to produce the results. Undoubtedly, other models could be devised that could also give similar results, but the strength of this particular one lies in its ability to mimic the kinetics of I_K with simple mechanisms and rate constants taken from voltage-clamp data in a straightforward manner.

In the results presented here, current waveforms were calculated for only one voltage. The rate constants should be voltage dependent, but because of difficulties in designing voltage-clamp paradigms to measure the voltage dependence of each rate constant and uncertainties of pharmacological separation of currents at different voltages (Thompson, 1977), no attempt has been made to elucidate the voltage dependence of each of the rate constants. Preliminary modeling indicates, however, that if the data on voltage dependence of inactivation, time-to-peak, and inactivation time-course presented elsewhere (Aldrich et al., 1979) are taken simply to reflect the voltage dependence of rate constants κ_r, α, and κ_a, respectively, a reasonable family of calculated current waveforms from voltage steps to between -30 and $+10$ mV can be obtained (Aldrich, 1979).

The four-state model for I_K is a departure from a traditional Hodgkin-Huxley type model for inactivating channels (Hodgkin and Huxley, 1952; Dodge, 1963; Frankenhaeuser, 1963; Connor and Stevens, 1971*c*). These models have all featured independence of inactivation and activation; the rate (or probability) of inactivation does not depend on the state of the channel (resting or activated). Models in which activation and inactivation are coupled have been presented by many authors for sodium channels (Hoyt, 1968; Goldman, 1976; Armstrong and Bezanilla, 1977) and for potassium channels inactivated by quaternary ammonium (Armstrong, 1969, 1975) and barium ions (Eaton and Brodwick, 1980; Armstrong and Taylor, 1980). In general, these models propose that only open channels can be inactivated, which leads to a dependence of inactivation upon activation. The four-state model for I_K presented here allows inactivation of both open and closed channels as in the Hodgkin-Huxley type

model, but activation and inactivation are coupled through the dependence of the probability of inactivation upon the state of the channel.

It has been shown that ions normally existing in the cell or its environment are capable of blocking potassium channels (Bergman, 1970; Bezanilla and Armstrong, 1972; French and Wells, 1977; Wanke et al., 1979; Moody, 1980). It is intriguing to examine the possibility that this could be a mechanism for inactivation of I_K. A simple formulation of the model based on this interpretation is that fast inactivation represents the voltage-dependent blocking of a resting channel. When a depolarizing voltage step is applied, one of two things can occur. The channel can be blocked by an inactivating particle (transition to state Z_r), or it can undergo a conformational change and allow ions to pass (transition to state A). After this conformational change, the probability of the channel being blocked is lessened, perhaps as a result of a change in the affinity of the binding site due to the conformational change. Open channels that bind the blocking particles undergo slow inactivation.

Additional states in the model may be required as more data are accumulated. In particular, the inclusion of at least one additional closed state is necessary to reproduce the sigmoid time course of activation of the current. Because analysis of the rising phase of the current is highly susceptible to errors due to incomplete isolation of the voltage-dependent current, and because the time-course of the rising phase shows great variability between preparations (Reuter and Stevens, 1980), the possibility of these other states is ignored in the solutions of the model presented here. Moreover, a transition between the two inactive states (Z_r and Z_a) may be required to explain more highly resolved components of recovery from inactivation. As presented here, the four-state model predicts a long current tail during recovery as inactivated channels in state Z_a return to rest through the activated state. Because of the slow time-course of recovery, however, the magnitude of this current would be extremely small and would not be resolvable, given the noise levels in our voltage-clamp records. At the present time, the four-state model accounts remarkably well for the features of inactivation of delayed rectification in molluscan neurons.

It is a pleasure to thank Dr. Stuart Thompson and Dr. Peter Getting for their support and encouragement. I also thank Richard Chailett, Drs. W. K. Chandler, C. F. Stevens, and R. W. Tsien for helpful suggestions on the manuscript.

This work was supported in part by training grant GM 07181 and grant NS 14519 from the National Institutes of Health to Stuart H. Thompson.

Received for publication 23 April 1981 and in revised form 15 July 1981.

REFERENCES

Adrian, R. H., W. K. Chandler, and A. L. Hodgkin. 1970*a*. Voltage clamp experiments in striated muscle fibres. *J. Physiol.* 208:607–644.

Adrian, R. H., W. K. Chandler, and A. L. Hodgkin. 1970*b*. Slow changes in potassium permeability in skeletal muscle. *J. Physiol.* 208:645–668.

Aldrich, R. W., Jr. 1979. Cumulative inactivation of delayed outward current in molluscan neurons and its role in use-dependent broadening of action potentials. Dissertation, Stanford University, Stanford, Calif.

Aldrich, R. W., P. A. Getting, and S. H. Thompson. 1979. Inactivation of delayed outward current in molluscan somata. *J. Physiol.* 291:507–530.

Alving, B. 1969. Differences between pacemaker and nonpacemaker neurons on voltage clamp. *J. Gen. Physiol.* 54:512–531.

Armstrong, C. M. 1969. Inactivation of the potassium conductance and related phenomena caused by quaternary ammonium ion injection in squid axons. *J. Gen. Physiol.* 54:553–575.

Armstrong, C. M. 1975. K pores of nerve and muscle membranes. *In* Membranes: A Series of Advances. G. Eisenman, editor. Marcel Dekker, Inc., New York. 3:325–358.

Armstrong, C. M., and F. Bezanilla. 1977. Inactivation of the sodium channel. II. Gating current experiments. *J. Gen. Physiol.* 70:567–590.

Armstrong, C. M., and S. R. Taylor. 1980. Interaction of barium ions with potassium channels in squid axons. *Biophys. J.* 30:473–488.

Bergman, C. 1970. Increase of sodium concentration near the surface of the nodal membrane. *Pflügers Arch. Eur. J. Physiol.* 317:287–302.

Bezanilla, F., and C. M. Armstrong. 1972. Negative conductance caused by entry of sodium and cesium ions into the potassium channel of squid axons. *J. Gen. Physiol.* 60:588–608.

Chandler, W. K., and H. Meves. 1970. Evidence for two types of sodium conductance in axons perfused with sodium fluoride solution. *J. Physiol.* 211:653–678.

Chiu, S. Y. 1977. Inactivation of sodium channels: second order kinetics in myelinated nerve. *J. Physiol.* 273:573–596.

Connor, J. A., and C. F. Stevens. 1971*a*. Inward and delayed outward membrane currents in isolated neural somata under voltage clamp. *J. Physiol.* 213:1–20.

Connor, J. A., and C. F. Stevens. 1971*b*. Voltage clamp studies of a transient outward current in gastropod neural somata. *J. Physiol.* 213:21–30.

Connor, J. A., and C. F. Stevens. 1971*c*. Prediction of repetitive firing behavior from voltage clamp data on an isolated neurone soma. *J. Physiol.* 213:31–53.

Dodge, F. A. 1963. A study of ionic permeability changes underlying excitation in myelinated nerve fibers of the frog. Dissertation, Rockefeller University, New York.

Eaton, D. C., and M. S. Brodwick. 1980. Effects of barium on the potassium conductance of squid axon. *J. Gen. Physiol.* 75:727–750.

Eckert, R., and H. D. Lux. 1977. Calcium-dependent depression of a late onward current in snail neurons. *Science (Wash. D.C.).* 197:472–475.

Ehrenstein, G., and D. L. Gilbert. 1966. Slow changes of potassium permeability in squid giant axon. *Biophys. J.* 6:553–566.

Frankenhaeuser, B. 1963. A quantitative description of potassium currents in myelinated nerve fibers of *Xenopus laevis*. *J. Physiol.* 169:424–430.

French, R. J., and J. B. Wells. 1977. Sodium ions as blocking agents and charge carriers in the potassium channels of the squid giant axon. *J. Gen. Physiol.* 70:707–724.

Gola, M. 1974. Neurones a ondes-salves des mollusques, variation cycliques lentes des conductances ioniques. *Pflügers Arch. Eur. J. Physiol.* 352:17–36.

Goldman, L. 1976. Kinetics of channel gating in excitable membranes. *Q. Rev. Biophys.* 9:491–526.

Hagiwara, S., K. Kusano, and N. Saito. 1961. Membrane changes of *Onchidium* nerve cell in potassium-rich media. *J. Physiol.* 155:470–489.

Heyer, C. B., and H. D. Lux. 1976*a*. Properties of a facilitating calcium current in pacemaker neurones of the snail, *Helix pomatia*. *J. Physiol.* 262:319–348.

Heyer, C. B., and H. D. Lux. 1976*b*. Control of the delayed outward potassium currents in bursting pacemaker neurons of the snail, *Helix pomatia*. *J. Physiol.* 262:349–382.

Hodgkin, A. L., and A. F. Huxley. 1952. A quantitative description of membrane current and its application to conduction and excitation in nerve. *J. Physiol.* 117:500–544.

Hoyt, R. C. 1968. Sodium inactivation in nerve fibers. *Biophys. J.* 8:1074–1097.

Kostyuk, P. G., O. A. Krishtal, and P. A. Doroshenko. 1975. Outward currents in isolated snail neurones. II. Effect of TEA. *Comp. Biochem. Physiol. C Comp. Pharmacol.* 54C:265–268.

Kostyuk, P. G., O. A. Krishtal, and P. A. Doroshenko. 1976. Outward currents in nerve cell membrane. *Bioelectrochem. Bioenerg.* 3:319–327.

Leicht, R., H. Meves, and H. H. Wellhoner. 1971. Slow changes of membrane permeability in giant neurones of *Helix pomatia*. *Pflügers Arch. Eur. J. Physiol.* 323:63–79.

Lux, H. D., and R. Eckert. 1974. Inferred slow inward current in neurones. *Nature (Lond.).* 250:574–576.

Magura, I. S., O. H. Krishtal, and A. G. Valeyev. 1971. Behavior of delayed current under long-duration voltage clamp in snail neurones. *Comp. Biochem. Physiol. A Comp. Physiol.* 40A:715–722.

Meech, R. W., and N. B. Standen. 1975. Potassium activation in *Helix aspersa* neurones under voltage clamp: a component mediated by calcium influx. *J. Physiol.* 249:211–239.

Moody, W., Jr., 1980. Appearance of calcium action potentials in crayfish slow muscle fibres under conditions of low intracellular pH. *J. Physiol.* 302:335–346.

Nakajima, S. 1966. Analysis of K inactivation and TEA action in the supramedullary cells of puffer. *J. Gen. Physiol.* 49:629–640.

Nakajima, S., S. Iwasaki, and K. Obata. 1962. Delayed rectification and anomalous rectification in frog's skeletal muscle membrane. *J. Gen. Physiol.* 46:97–115.

Neher, E. 1971. Two fast transient current components during voltage clamp on snail neurons. *J. Gen. Physiol.* 59:36–53.

Neher, E., and H. D. Lux. 1971. Properties of somatic membrane patches of snail neurons under voltage clamp. *Pflügers Arch. Eur. J. Physiol.* 322:35–38.

Reuter, H., and C. F. Stevens. 1980. Ion conductances and ion selectivity of potassium channels in snail neurones. *J. Membr. Biol.* 57:103–118.

Schwarz, J. R., and W. Vogel. 1971. Potassium inactivation in single myelinated nerve fibers of *Xenopus laevis*. *Pflügers Arch. Eur. J. Physiol.* 330:61–73.

Thompson, S. H. 1977. Three pharmacologically distinct potassium channels in molluscan neurones. *J. Physiol.* 265:465–488.

Wanke, E., E. Carbone, and P. L. Testa. 1979. K^+ conductance modified by a titratable group accessible to protons from the intracellular side of the squid axon membrane. *Biophys. J.* 26:319–324.